Seasonal Variations in the Circulation over the Middle Atlantic Bight Continental Shelf

STEVEN J. LENTZ

Woods Hole Oceanographic Institution, Woods Hole, Massachusetts

(Manuscript received 24 January 2007, in final form 20 November 2007)

ABSTRACT

Fits of an annual harmonic to depth-average along-shelf current time series longer than 200 days from 27 sites over the Middle Atlantic Bight (MAB) continental shelf have amplitudes of a few centimeters per second. These seasonal variations are forced by seasonal variations in the wind stress and the cross-shelf density gradient.

The component of wind stress that drives the along-shelf flow over most of the MAB mid- and outer shelf is oriented northeast–southwest, perpendicular to the major axis of the seasonal variation in the wind stress. Consequently, there is not a significant seasonal variation in the wind-driven along-shelf flow, except over the southern MAB shelf and the inner shelf of New England where the wind stress components forcing the along-shelf flow are north–south and east–west, respectively.

The seasonal variation in the residual along-shelf flow, after removing the wind-driven component, has an amplitude of a few centimeters per second with maximum southwestward flow in spring onshore of the 60-m isobath and autumn offshore of the 60-m isobath. The spring maximum onshore of the 60-m isobath is consistent with the maximum river discharges in spring enhancing cross-shelf salinity gradients. The autumn maximum offshore of the 60-m isobath and a steady phase increase with water depth offshore of Cape Cod are both consistent with the seasonal variation in the cross-shelf temperature gradient associated with the development and destruction of a near-bottom pool of cold water over the mid and outer shelf ("cold pool") due to seasonal variations in surface heat flux and wind stress.

1. Introduction

There is a mean equatorward along-shelf flow of 5–10 cm s^{-1} over the continental shelf of the Middle Atlantic Bight (MAB) and southern flank of Georges Bank (e.g., Bumpus 1973; Beardsley and Boicourt 1981; Butman and Beardsley 1987; Lentz 2008). One might expect a corresponding seasonal variation (annual cycle) in the along-shelf flow because there are well-documented seasonal variations in both the wind stress (Saunders 1977) and in the structure of the density field (Bigelow 1933; Bigelow and Sears 1935; Beardsley et al. 1985; Flagg 1987; Linder and Gawarkiewicz 1998). However, the magnitude, pattern, and cause of seasonal variations in the circulation of the MAB remain unclear.

There is clear evidence of a seasonal variation in the along-shelf flow over the southern flank of Georges Bank with an amplitude of a few centimeters per second and maximum southwestward along-shelf flow in September (Butman and Beardsley 1987; Brink et al. 2003; Flagg and Dunn 2003). Shearman and Lentz (2003) observed a maximum monthly mean along-shelf flow of about 10 cm s^{-1} in September 1996, decreasing to a few centimeters per second in spring 1997 over the mid and outer New England shelf. However, several previous studies of mid and outer-shelf currents in the same region did not observe a well-defined seasonal variation in the along-shelf flow (Mayer et al. 1979; Beardsley et al. 1985; Aikman et al. 1988). In an analysis of current profiles from 10 years of weekly cross-shelf transects between New York and Bermuda, Flagg et al. (2006) observed a large seasonal variation in the shelf–slope jet offshore of the 100-m isobath, with strongest along-slope flow in winter (20 cm s^{-1}) and weaker flow in spring–summer (10 cm s^{-1}). Linder and Gawarkiewicz (1998) observed a similar seasonal variation in geostrophic estimates of shelf–slope jet transport south of Cape Cod. However, Flagg et al. (2006) observed "little seasonal variation" in the along-shelf flow onshore of the shelf–slope jet (water depths less

Corresponding author address: Steven J. Lentz, Woods Hole Oceanographic Institution, MS 21, Woods Hole, MA 02543.
E-mail: slentz@whoi.edu

DOI: 10.1175/2007JPO3767.1

© 2008 American Meteorological Society

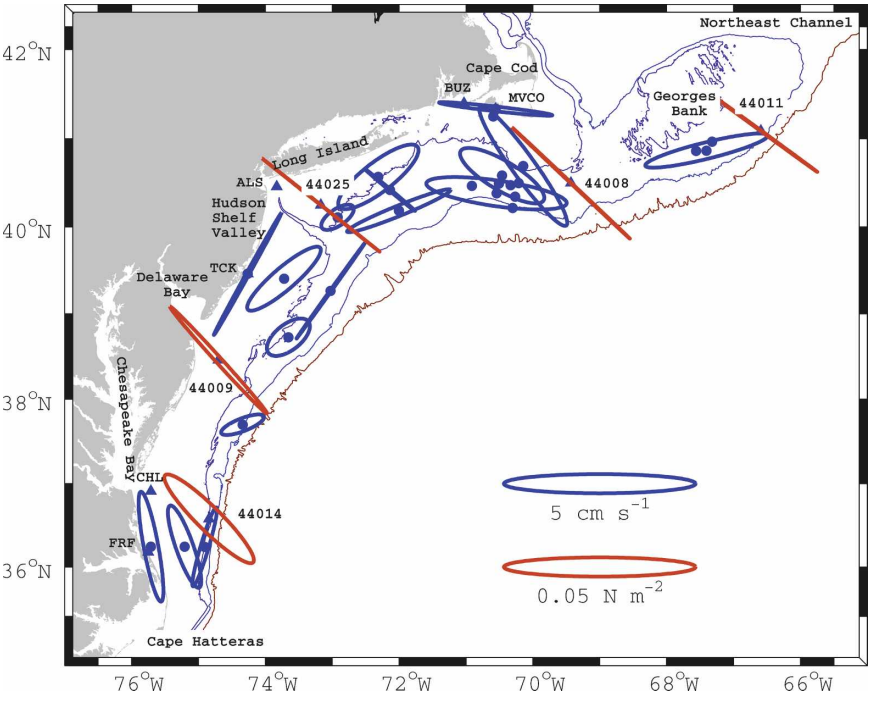

FIG. 1. Map of the Middle Atlantic Bight showing the locations of the current-meter mooring sites (solid circles), wind stations (solid triangles), and seasonal ellipses for depth-averaged currents (blue) and wind stress (red). Not all ellipses are shown for clarity. The 50-, 100-, and 1000-m isobaths are shown.

than 100 m). Ullman and Codiga (2004) and Codiga (2005) observed a substantial seasonal variation in the along-shelf flow over the inner shelf near the mouth of Long Island Sound. In contrast to the outer-shelf sites listed above, the along-shelf flow at this inner-shelf site was strongest in summer and weak, or nonexistent, in winter.

Seasonal variations in the along-shelf flow over the MAB shelf have often been attributed to seasonal variations in the cross-shelf density gradient (Butman 1987; Shearman and Lentz 2003; Flagg et al. 2006). Ullman and Codiga (2004) and Codiga (2005) found that wind forcing also contributed to seasonal variations in the along-shelf flow over the inner shelf near Long Island Sound. Several sources of seasonal variation in the cross-shelf density structure have been identified. In the vicinity of the 50-m isobath over Georges Bank, the seasonal variation in the cross-shelf density gradient is associated with the establishment of a tidal mixing front in spring and summer (Flagg 1987). Over the New England shelf, Shearman and Lentz (2003) argue that seasonal variations in the temperature structure associated with surface heating and cooling (Bigelow 1933; Beardsley and Boicourt 1981) cause seasonal variation in the cross-shelf density gradient. Ullman and Codiga (2004) and Codiga (2005) found that cross-shelf density gradients over the inner shelf near Long Island Sound are associated with buoyant outflow from Long Island Sound.

The goal of this study is to determine whether there is a consistent pattern to seasonal variations in the MAB circulation and, if so, what drives the seasonal variability. To address these questions, an annual cycle is fit to current time series longer than 200 days from 27 sites over the continental shelf of the MAB and southern flank of Georges Bank. The analysis indicates that there are significant seasonal variations in the along-shelf flow associated with seasonal variations in both the wind stress and the cross-shelf density gradient.

2. Observations and processing

a. Observations

The 27 sites with long current records span the inner, mid, and outer shelf, but the spatial coverage is sparse and the along-shelf distribution is not uniform, with many of the stations concentrated over the New England shelf (Fig. 1; Table 1). In particular, there are relatively few sites south of the Hudson shelf valley, which extends across the shelf. Three sites from the southern flank of Georges Bank are included because the shelf is continuous with the mid- and outer MAB

TABLE 1. Summary of annual harmonic analysis of 27 along-shelf current time series. Positions, water depth h, instrument depth z when an interior velocity is used instead of the depth-averaged "da" flow, and length of time series are included. Orientation is relative to true north and phase is zero on 1 Jan. Error bars are 95% confidence intervals. Major and minor axis error bars, and orientation and phase error bars are the same.

Latitude (°N)	Longitude (°W)	h (m)	z (m)	Length (days)	Major (cm s^{-1})	Minor (cm s^{-1})	Orientation (°N)	Phase (°)
40°51.8′	67°33.5′	76	da	204	3.0	−1.1 ± 4.0	55.3	353.3 ± 95.3
40°58.1′	67°19.2′	75	da	827	2.1	0.7 ± 1.8	119.0	217.9 ± 56.5
40°52.1′	67°24.3′	81	45	1065	3.3	−0.4 ± 1.5	76.2	72.1 ± 27.0
41°20.2′	70°33.4′	12	da	1577	3.0	0.1 ± 1.2	96.4	180.0 ± 22.8
41°19.1′	70°34.2′	18	da	276	2.6	0.1 ± 3.2	87.7	24.0 ± 70.2
41°15.2′	70°35.5′	28	da	372	4.7	0.2 ± 1.5	100.9	200.1 ± 17.8
40°41.6′	70°8.6′	46	32	348	3.8	0.6 ± 2.7	144.1	201.1 ± 41.7
40°30.0′	70°12.5′	66	32	424	0.9	−0.1 ± 2.7	164.1	256.9 ± 174.0
40°20.6′	70°16.1′	88	32	393	1.7	1.0 ± 2.7	48.6	194.8 ± 158.9
40°12.9′	70°18.2′	105	59	393	3.5	−0.7 ± 2.7	65.0	199.1 ± 47.6
40°28.0′	70°54.7′	80	da	379	3.8	−0.3 ± 2.8	76.9	49.0 ± 43.2
40°35.0′	70°27.5′	64	da	302	2.5	0.8 ± 3.2	120.8	244.7 ± 84.3
40°29.5′	70°30.3′	70	da	310	3.9	0.6 ± 3.2	109.8	258.4 ± 49.7
40°23.0′	70°32.6′	86	da	310	3.7	0.7 ± 3.2	98.1	284.8 ± 52.3
40°28.5′	70°20.1′	70	50	310	3.8	−0.3 ± 3.2	94.3	246.5 ± 48.4
40°34.2′	72°18.5′	49	da	473	2.6	−0.8 ± 1.3	52.5	145.2 ± 32.4
40°25.3′	72°8.2′	59	da	213	1.7	−0.0 ± 1.3	129.9	5.9 ± 42.7
40°11.1′	72°0.2′	65	da	335	2.9	−0.3 ± 1.3	68.0	1730.8 ± 25.3
40°6.6′	72°55.2′	47	da	818	1.0	0.4 ± 1.3	55.7	341.8 ± 99.7
39°15.9′	73°1.4′	70	da	261	3.1	0.0 ± 1.3	35.6	140.1 ± 23.8
39°24.3′	73°43.2′	32	da	416	2.5	0.6 ± 1.3	49.5	115.2 ± 31.8
39°27.7′	74°15.7′	11	da	510	3.6	0.1 ± 1.8	29.0	287.3 ± 29.0
38°43.6′	73°39.3′	61	da	720	1.3	−0.7 ± 1.9	51.7	315.6 ± 122.1
37°42.0′	74°20.4′	90	da	399	1.2	−0.3 ± 2.7	68.7	108.1 ± 144.4
36°14.7′	75°42.5′	22	16	536	2.9	−0.4 ± 2.1	−10.4	209.1 ± 41.5
36°14.7′	75°12.4′	35	20	461	2.3	−0.5 ± 2.1	−19.5	217.3 ± 55.1
36°14.6′	74°54.4′	60	30	560	2.1	0.2 ± 2.1	16.5	309.5 ± 55.7

shelf. Vertical coverage at each site varies substantially from acoustic Doppler current profilers (ADCPs) with bins every meter or less over about 80% of the water column to moorings with as few as two current meters (Table 1). For sites with sufficient vertical coverage, depth-averaged flows are estimated using a trapezoidal integration and assuming the flow is vertically uniform near the boundaries to extrapolate to the surface and bottom. Results are similar if the velocity profile is extrapolated linearly to the surface and bottom. For sites where accurate estimates of the depth-average flow are not possible, because of short records at some depths or only a few instruments in the vertical, interior currents are used to represent the along-shelf flow (Table 1).

To characterize the wind forcing, observations from five National Data Buoy Center (NDBC) buoys, three towers, and three coastal masts spanning the MAB and southern flank of Georges Bank are analyzed (Fig. 1; Table 2). The wind time series are 10–20 yr long, with the exception of two coastal sites: Martha's Vineyard Coastal Observatory (MVCO) south of Cape Cod and Tuckerton (TCK), New Jersey. The NDBC buoys are located over the mid- to outer shelf. The Buzzards Bay (BUZ) west of Cape Cod, Ambrose (ALS) in New York Bight, and Chesapeake Bay (CHL) towers are over the inner shelf. The MVCO and Tuckerton masts are at the coast and the mast at the Army Corps Field Research Facility (FRF) near Duck, North Carolina, is at the end of a pier. Wind stresses are estimated from wind velocities and sensor heights using a bulk formula (Large and Pond 1981).

Historical hydrographic observations from the National Oceanographic Data Center's (NODC's) World Ocean Database 2001 archive of ship observations are used to characterize the seasonal variation in the cross-shelf structure of temperature, salinity, and density. The observations were quality controlled and water depths were determined using the National Geophysical Data Center high-resolution bathymetry for the region (Lentz et al. 2003). A total of 20 158 profiles over the shelf (water depth ≤100 m) were extracted, excluding profiles in Chesapeake Bay, Delaware Bay, Long Island Sound, Buzzards Bay, and Nantucket Sound. Each shelf profile was interpolated onto a 5-m vertical grid.

TABLE 2. Summary of annual harmonic analysis of wind stresses. Orientation is relative to true north and phase is zero on 1 Jan. Error bars are 95% confidence intervals on estimates.

Station	Latitude (°N)	Longitude (°W)	Duration (yr)	Major axis (10^{-2} N m^{-2})	Minor axis (10^{-2} N m^{-2})	Orientation (from N)	Phase (°)
44011	41°5.4′	66°35.4′	16.4	3.6 ± 0.5	0.0 ± 0.4	143.9 ± 7.0	186.9 ± 7.9
MVCO	41°20.2′	70°33.4′	5.1	1.1 ± 0.4	−0.2 ± 0.4	141.0 ± 20.9	191.0 ± 20.2
BUZ	41°24.0′	71°1.8′	18.6	4.3 ± 0.6	−0.6 ± 0.6	148.2 ± 7.9	181.3 ± 8.0
44008	40°30.0·′	69°25.8′	18.9	4.2 ± 0.6	0.0 ± 0.6	136.7 ± 7.7	184.3 ± 7.7
ALS	40°27.6′	73°49.8′	19.6	3.5 ± 0.4	0.1 ± 0.4	128.7 ± 6.9	188.3 ± 6.6
44025	40°15.0′	73°10.2′	17.6	3.9 ± 0.4	0.0 ± 0.4	141.6 ± 5.6	182.5 ± 6.1
TCK	39°27.7′	74°15.7′	2.1	1.3 ± 0.5	−0.4 ± 0.4	115.2 ± 21.0	196.2 ± 23.9
44009	38°27.6′	74°42.0′	17.0	3.8 ± 0.5	0.2 ± 0.6	132.3 ± 8.6	182.1 ± 8.2
CHL	36°54.6′	75°42.6′	17.5	3.7 ± 0.5	1.2 ± 0.4	119.1 ± 7.5	171.0 ± 8.9
FRF	36°10.8′	75°45.0′	22.0	1.5 ± 0.3	0.6 ± 0.3	100.8 ± 12.6	175.4 ± 14.8
44014	36°34.8′	74°50.4′	11.8	3.2 ± 0.5	0.6 ± 0.5	135.3 ± 9.5	182.8 ± 9.5

Seasonal variations in near-bottom cross-isobath density differences $\Delta\rho_b$ and temperature differences ΔT_b were estimated as follows using the historical hydrographic profiles from the NODC archive: First, the average for each day of the year of all density (or temperature) observations within 20 m of the bottom, in a 20-m water depth band centered on a given isobath, were computed for 10-m isobath intervals from 10 to 120 m. Then a seasonal cycle was fit to the density differences between adjacent isobath bins. Seasonal variations in ΔT_b were also determined from a few concurrent mooring pairs over the New England and southern MAB shelf.

b. Harmonic analysis and uncertainty estimates

Seasonal cycles of currents, wind stresses, and cross-shelf temperature and density gradients are estimated by fitting observations to a mean and annual harmonic:

$$y(t) = \bar{y} + a\sin\omega t + b\cos\omega t,$$

where y is a time series, t is time in days, $\bar{y}$ is the time average, $\omega = 2\pi/(365.25\ \text{day})^{-1}$ is the annual frequency, and a and b are coefficients of the harmonic fit. For scalar time series results of the harmonic analysis can be summarized as an amplitude and phase of the annual cycle. For vector time series, the a and b coefficients are complex and the results are summarized in terms of an ellipse characterized by the major and minor axes, the orientation of the major axis, and the phase. The following analysis focuses on the depth-averaged along-shelf flow. Phases are presented as the time of year when the equatorward flow (direction of the mean flow) is a maximum.

Uncertainties in a and b are determined using the residual current variance in a low-frequency band around the annual frequency ω and assuming Gaussian statistics. Uncertainties in the corresponding amplitude and phase or ellipse characteristics are then determined through a linearized error analysis. This is the same procedure used to estimate uncertainties in tidal constituents (Pawlowicz et al. 2002).

The error analysis can be applied directly to the wind stress time series because they are typically 10–20 yr long. Individual current time series are too short to accurately estimate the spectral variance of the residual time series in the frequency band around the annual frequency. Examination of the current spectra from the few sites with longer time series indicates the spectral density in the along-shelf component of the flow is $\sim 10^4$ (cm s^{-1})^2 (cpd)$^{-1}$. Therefore, uncertainties in the current amplitudes and phases at all sites are estimated assuming this value for the spectral density of the residual flow in the frequency band around the annual frequency. The current time series are also too short (200 days to 3 yr) to determine whether there is a consistent seasonal cycle over many years at individual sites. Therefore, confidence in the generality of the results is based on the consistency of the patterns observed for all the sites, and the results are only suggestive with regard to a consistent seasonal cycle.

3. Seasonal variations

a. Wind stress

In winter, the MAB is in the westerly wind band (Isemer and Hasse 1985) and the mean winds are relatively strong toward the southeast. From spring to summer, the subtropical high over the North Atlantic strengthens and moves northward, displacing the westerlies, resulting in weak northwestward mean winds in summer. As a result, wind stresses in the MAB exhibit a significant, spatially uniform annual cycle (Fig. 1 and Table 2). The amplitude of the major axis seasonal

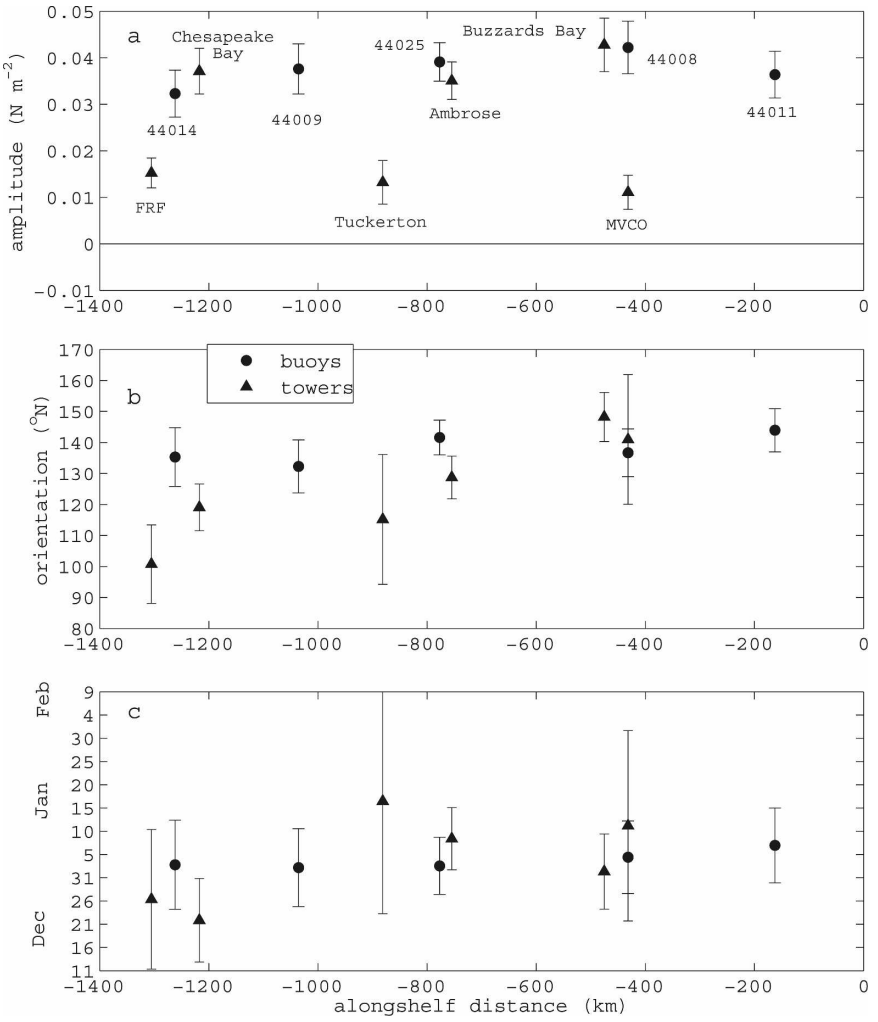

FIG. 2. Major axis (a) amplitude and (b) orientation and (c) phase of wind stress seasonal ellipses as a function of along-shelf distance from northeastern Georges Bank (0 km) to Cape Hatteras (−1400 km). Orientations are relative to true north and phases are date of maximum southeastward wind stress. Error bars indicate 95% confidence interval for estimates.

variation is 0.03–0.04 N m^{-2} at all the sites except that the three coastal masts have substantially smaller amplitudes, 0.01–0.015 N m^{-2} (Fig. 2a). The amplitudes are reduced at the coast because the mean and seasonal winds are offshore so that there are topographic effects such as flow separation and the surface roughness over land is generally larger than over water (e.g., Vickers et al. 2001). Thermodynamic adjustment in the marine boundary layer may also be important (e.g., Austin and Lentz 1999). The cross-shore distance over which the amplitude of the seasonal cycle increases to the shelf values is not known but is probably 10 km or less since the Buzzards Bay, Ambrose, and Chesapeake Light towers are all close to shore but have amplitudes similar to the offshore buoys. Consequently, buoy winds are used in place of the three coastal wind stations when determining the wind-driven response of the circulation.

Minor axis amplitudes are not significantly different from zero except in the southern MAB (Fig. 1; Table 2). The seasonal variation in wind stress is polarized in the southeast to northwest direction (orientation ~135°N; Fig. 2b), with the maximum southeastward wind stress in early January (Fig. 2c) and maximum northwestward wind stress in June. Both the phase and orientation are essentially the same throughout the MAB. The mean wind stress is toward the southeast with a magnitude of 0.02–0.03 N m^{-2}, so the seasonal variation reinforces the mean wind stress in winter and opposes the mean wind stress in summer. Since the

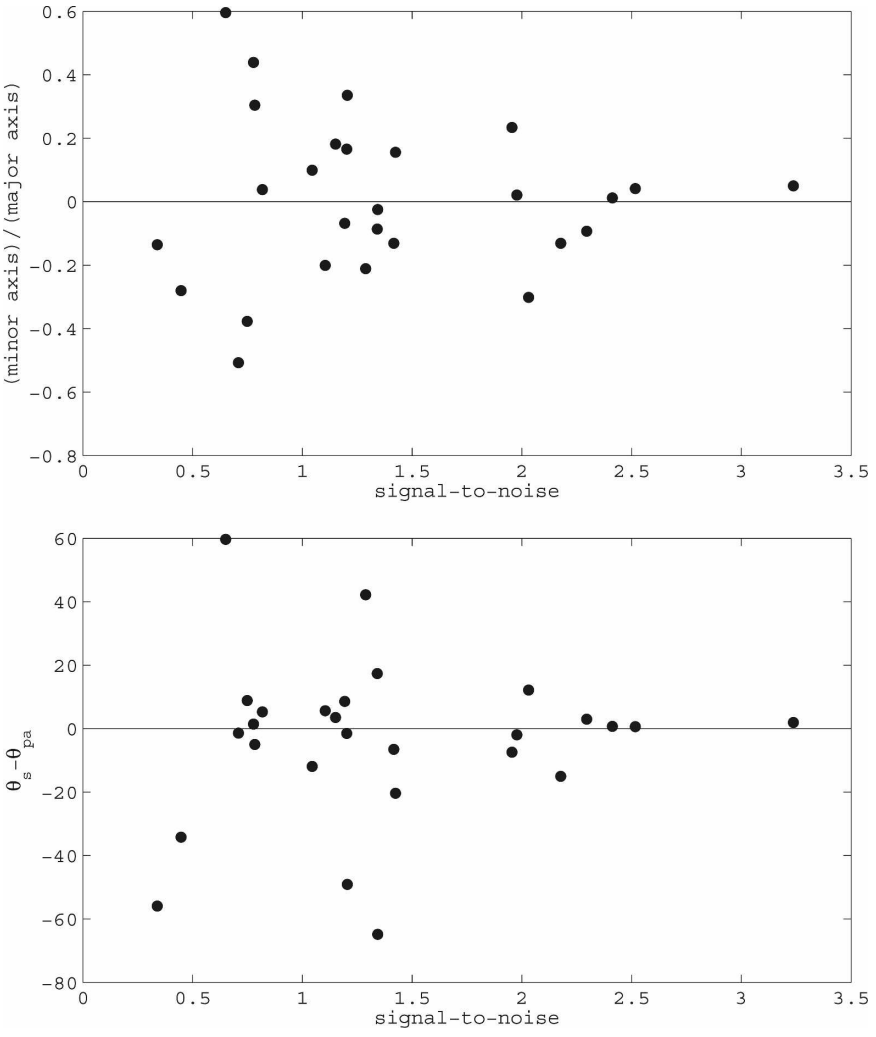

FIG. 3. (a) Ratio of minor to major axes of seasonal current ellipses and (b) seasonal ellipse orientation (θ_s) relative to principal axes of subtidal flow (θ_{pa}) both as a function of signal-to-noise (ratio of major axis to uncertainty in major axis).

minor axis is approximately zero, there is not a significant seasonal variation in the northeast to southwest wind stress component (orientation ~45°N). This has important consequences for the seasonal variations in the wind-driven circulation over the MAB shelf because the along-shelf flow is driven by the northeast–southwest component of the wind stress over much of the MAB shelf.

b. Depth-average (interior) currents

Seasonal variations in the depth-average (or interior) flow are polarized at all sites (Figs. 1 and 3), with major axis amplitudes of 1–5 cm s^{-1} (Table 1). The amplitudes are significantly different from zero at the 95% confidence level for 18 of the 27 time series. The uncertainties tend to be large relative to the amplitudes because the time series are only about 1 yr long. The orientation of the seasonal variation is generally aligned with the principal axes of the subtidal flow, which is along-isobath, though there are exceptions (Figs. 3b and 1). Minor axis (cross-isobath) amplitudes are all insignificant at the 95% confidence level (Table 1). The remaining analyses focus on the depth-average along-shelf flow, where along-shelf is defined as the orientation of the major axes of the subtidal flow, positive poleward. No consistent pattern was found for seasonal variations in the cross-shelf component of flow at any depth, probably because the uncertainties are large relative to the amplitudes of the seasonal variations for these short time series.

Amplitudes of the seasonal variation in the depth-

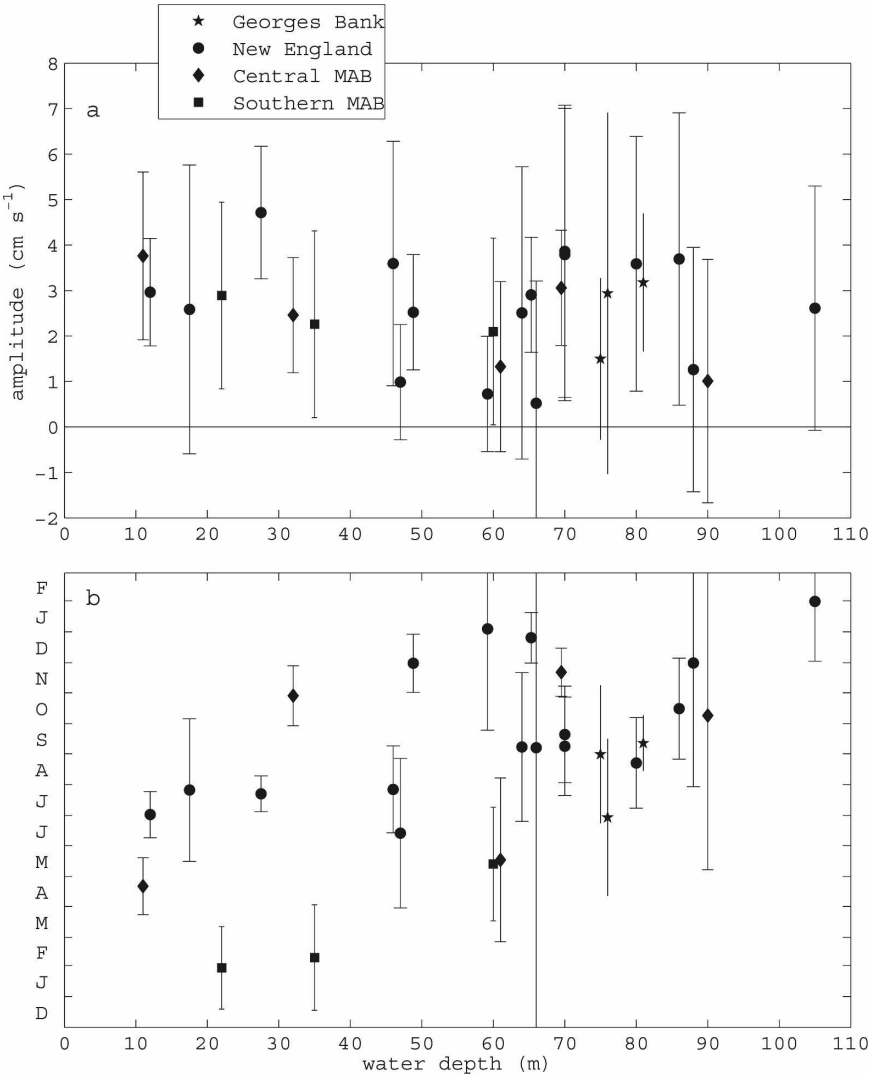

FIG. 4. (a) Major axis amplitude and (b) phase of along-shelf current from harmonic analysis as a function of water depth. Phases are time (month) of maximum equatorward flow. Error bars indicate 95% confidence interval for estimates. Minor axis amplitudes (not shown) are not significantly different from zero for any of the time series (Table 1).

average along-shelf flow are 1–5 cm s^{-1} with no clear dependence on water depth or along-shelf position (Fig. 4a). There are large variations in the time of maximum equatorward along-shelf flow (phase) with a tendency for the phase to increase with increasing water depth (Fig. 4b). The seasonal variations in the along-shelf flow consist of at least two components: a wind-driven component associated with seasonal variations in the wind stress and a buoyancy-driven component associated with seasonal variations in the cross-shelf density gradient. Therefore, the wind-driven component is examined first and then removed from the current time series to isolate the buoyancy-driven component.

c. Along-shelf current response to wind forcing

Along-shelf currents at all 27 sites are significantly correlated with the wind stress (correlations 0.5–0.8). However, there are substantial spatial variations in the along-shelf current response to the wind stress forcing. Both the amplitude of the response to the wind stress (Noble et al. 1983) and the orientation of the wind stress that is most correlated with the along-shelf currents (Beardsley et al. 1985; Shearman and Lentz 2003; Kohut et al. 2004) vary within the MAB. Regression coefficients between the wind stress and the subtidal depth-averaged along-shelf flow increase by a factor of 2 or more from Georges Bank to the southern MAB

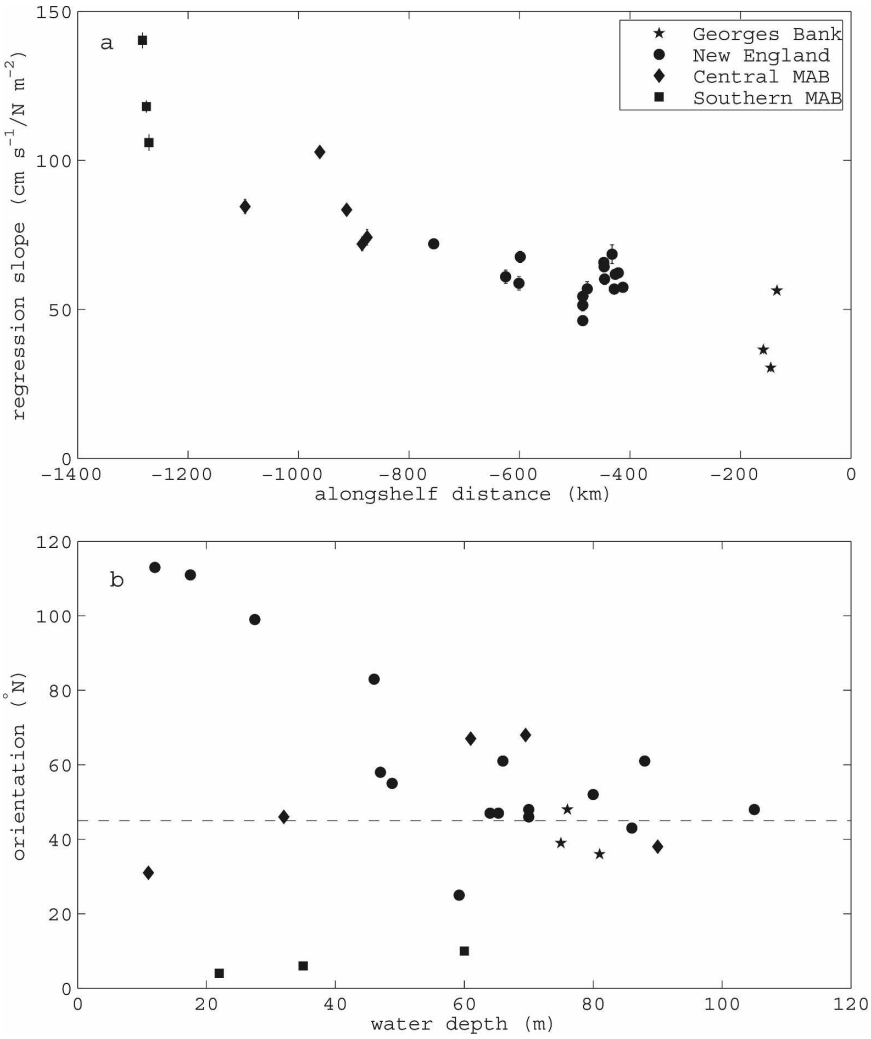

FIG. 5. (a) Slope of linear regression as a function of along-shelf distance from northeastern Georges Bank (0 km) to Cape Hatteras (−1400 km). Linear regression is $v^{da} = a\tau^s + b$, where a is the slope and b (not shown) is the intercept, and τ^s is the component of the wind stress that yields the maximum correlation with v^{da}. (b) Orientation of the wind stress that yields the maximum correlation with v^{da} as a function of water depth. Dashed line indicates orientation of wind stress component without a seasonal variation. Error bars in (a) indicate 95% confidence interval.

(Fig. 5a). The wind stress orientation that yields maximum correlation with the along-shelf flow is approximately north–south (10°–20°N, solid square in Fig. 5b) south of Chesapeake Bay, east–west (90°–110°N) near the coast south of Martha's Vineyard (solid circle: water depths less than 60 m), and northeast–southwest (30°–70°N) at all the other sites (Georges Bank, mid and outer New England shelf, and the central MAB).

The wind-driven flow was estimated by rotating the wind stress to the orientation of maximum correlation (Fig. 5b) and multiplying by the regression coefficient (Fig. 5a) for each site. The seasonal variation of the estimated wind-driven flow was then calculated for each site. The regression coefficient and orientation based on subtidal values are used because regression coefficients and orientations based on monthly values are similar, but less certain, since there are fewer degrees of freedom. Monthly values of the estimated wind-driven flow are generally significantly correlated with monthly average along-shelf flows.

There is not a significant seasonal variation in the wind-driven along-shelf flow at most sites (Fig. 6) because the component of the wind stress that drives the depth-averaged along-shelf flow (40°–60°N in Fig. 5b) is perpendicular to the orientation of the seasonal variation in the wind stress (130°–150°N in Fig. 2b). In

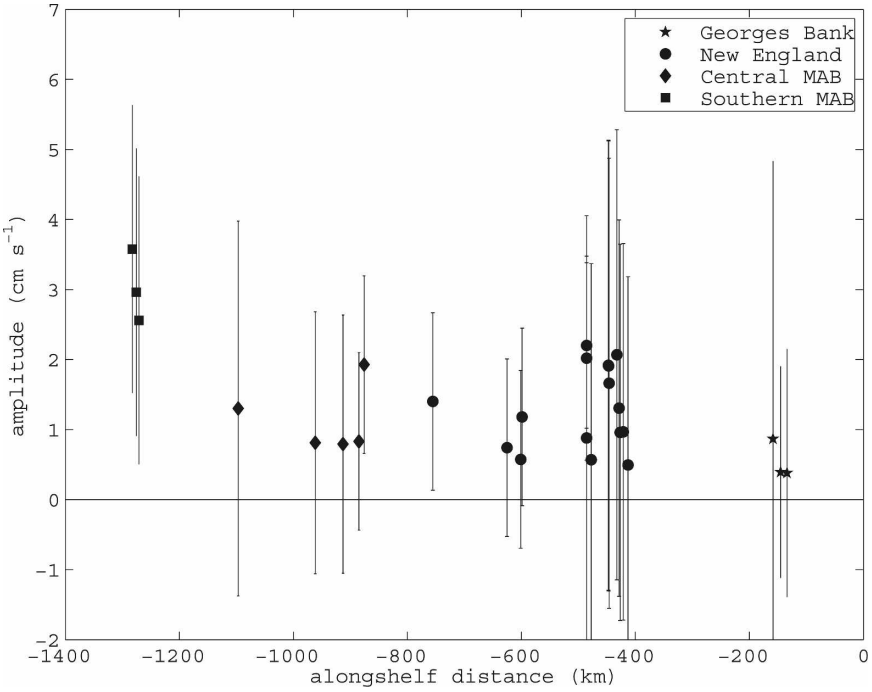

FIG. 6. Amplitude of the seasonal cycle of the wind-driven depth-average along-shelf flow as a function of along-shelf distance from northeastern Georges Bank (0 km) to Cape Hatteras (−1400 km). Error bars indicate 95% confidence interval for estimates.

particular, in water depths greater than 60 m, the amplitudes of the seasonal variation in the estimated wind-driven flow are 2 cm s^{-1} or less (not shown) and are not significantly different from zero at the 95% confidence level.

In the southern MAB, where the regression slope is large (solid square: Fig. 5a) and the orientation of the wind stress that drives the depth-averaged along-shelf flow is roughly north–south (solid square: Fig. 5b), the wind drives a significant seasonal variation in the depth-averaged along-shelf flow of about 3 cm s^{-1} with maximum southward along-shelf flow in winter (solid square: Fig. 6).

Over the New England shelf, south of Cape Cod, the orientation of the wind stress that drives the depth-averaged along-shelf flow rotates from east–west over the inner shelf to northeast–southwest over the middle and outer shelf (solid circle: Fig. 5b). Consequently, there is a significant seasonal variation of 2 cm s^{-1} with maximum westward along-shelf flow in summer over the inner shelf that decreases offshore (Figs. 6 and 7). Year-to-year variations in the monthly average currents over the mid and outer shelf are large (Figs. 7c,d). This is due in part to the impact of individual storm events on the monthly values and emphasizes the need for much longer time series to accurately determine seasonal cycles in the circulation.

d. Current response related to cross-shelf buoyancy gradients

Estimates of the subtidal wind-driven flow were subtracted from the current time series at each site and the seasonal harmonic analysis was applied to the residual time series. Amplitudes of the seasonal harmonic of the residual along-shelf flow range from 1 to 5 cm s^{-1} and only about half of the amplitudes are significantly different from zero (Fig. 8a). The amplitudes do not exhibit any obvious systematic dependence on water depth (offshore distance) or along-shelf position, though any such pattern may be obscured by the large uncertainties in the estimates.

The phases tend to fall into two groups (Fig. 8b). Onshore of the 60-m isobath, maximum equatorward flow tends to occur in the spring (February–June), particularly for sites west of 72°W (open symbols Fig. 8b). This is consistent with the timing of maximum freshwater discharge from MAB estuaries (discussed below). Offshore of the 60-m isobath maximum equatorward flow tends to occur in the autumn (September–December). For sites south of Cape Cod (solid circle: Fig. 8b) there is a steady phase increase with water depth from May in shallow water to December–January near the shelf break. The offshore fall maximum and the phase increase with increasing water depth south of Cape Cod

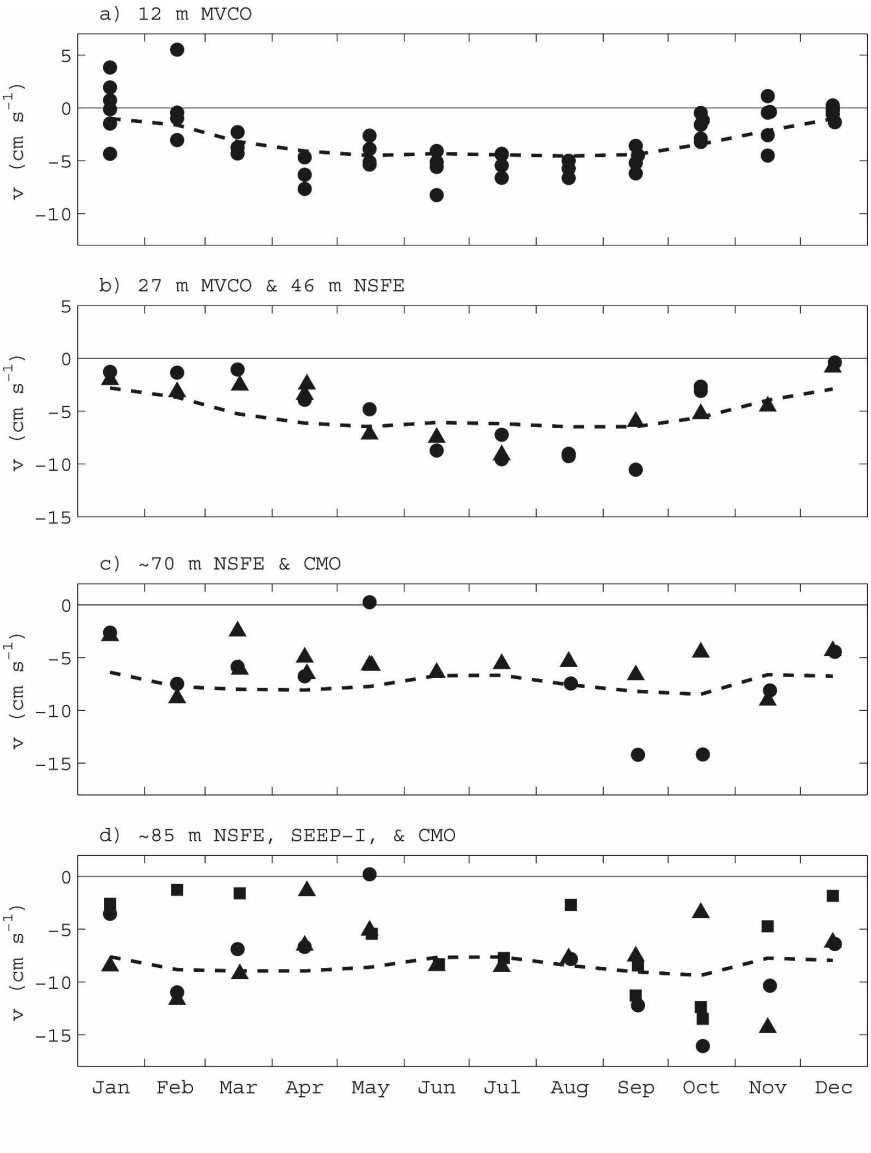

FIG. 7. Monthly averages of the depth-average or interior along-shelf flow v over the New England shelf at (a) 12-m water depth, (b) 27-m (circle) and 46-m (triangle) water depth, (c) ~70-m water depth, and (d) ~85-m water depth. The estimated wind-driven along-shelf flow for each site is also shown (dashed lines).

are both consistent with the along-shelf flow being in thermal wind balance with the cross-shelf density gradient (Lentz et al. 1999; Shearman and Lentz 2003; Garvine 2004; Codiga 2005) and the tendency for the maximum near-bottom cross-isobath temperature differences to occur later in the year in deeper water (discussed below).

There is a relatively strong cross-shelf salinity gradient over the MAB shelf with fresher water near the coast (Fig. 9). However, the seasonal variations in both salinity (Manning 1991; Mountain 2003) and the cross-shelf salinity gradient (Shearman and Lentz 2003) tend to be small, except over the inner shelf where there can be an enhanced cross-shelf salinity gradient due to spring runoff (March–April: Fig. 9) (Ullman and Codiga 2004; Codiga 2005). The maximum equatorward flow in spring onshore of the 60-m isobath and west of 72°W (open symbols: Fig. 8b) may be associated with spring runoff enhancing the cross-shelf density gradient over the inner shelf. The Connecticut River is located at about 72°W and has a well-documented impact on seasonal variations in the flow in that area (Ullman and

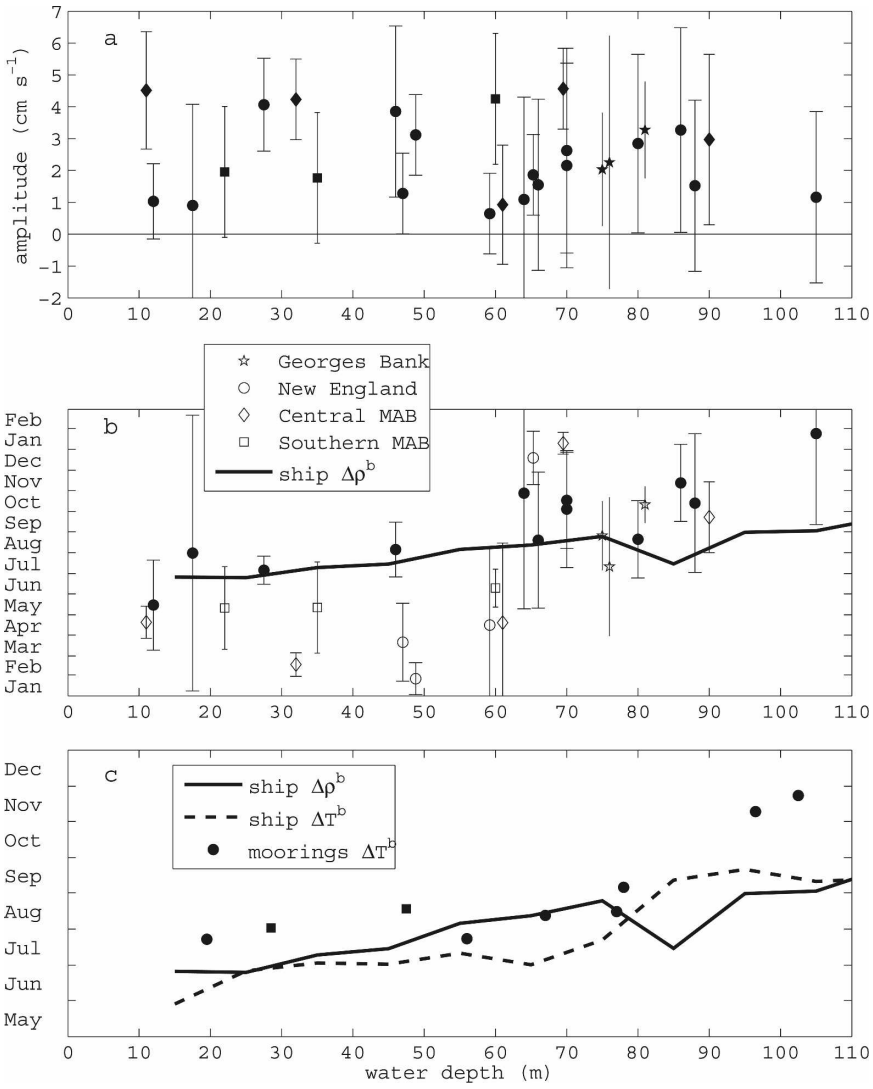

FIG. 8. (a) Amplitude and (b) phase of the seasonal ellipse of the residual depth-averaged along-shelf flow when the wind-driven flow is removed as a function of water depth. The phase of the near-bottom cross-shelf temperature or density difference is shown in (c). Error bars indicate 95% confidence interval for estimates.

Codiga 2004; Codiga 2005). The Hudson River, Delaware Bay, and Chesapeake Bay all have peak freshwater discharges in spring. The associated buoyant coastal currents reduce the inner-shelf salinity, increasing the cross-shelf density gradient, and enhance the along-shelf flow (e.g., Munchow and Garvine 1993; Rennie et al. 1999; Yankovsky et al. 2000).

There is a large seasonal variation in the cross-shelf temperature gradient (Fig. 10; Shearman and Lentz 2003). In winter (December–March), thermal stratification is weak and the shelf water temperatures decrease onshore because of surface cooling. In winter, the cross-shelf temperature gradient (denser water near the coast) opposes the cross-shelf salinity gradient (lighter water near the coast), resulting in a reduced cross-shelf density gradient. Surface heating in the spring leads to the development of a shallow seasonal thermocline that isolates a region of residual cold winter water near the bottom over the mid and outer shelf, called the "cold pool," that persists from May through October (Fig. 10: Bigelow 1933; Houghton et al. 1982). Note this is not simply a local response. The cold-pool water is advected equatorward along-shelf by the mean flow and hence comes from regions to the north (Houghton et al. 1982). Offshore of the center of the cold pool, the near-bottom cross-shelf temperature gradient continues to oppose the cross-shelf salinity gradient, as in winter. However, onshore of the cold pool, the near-bottom

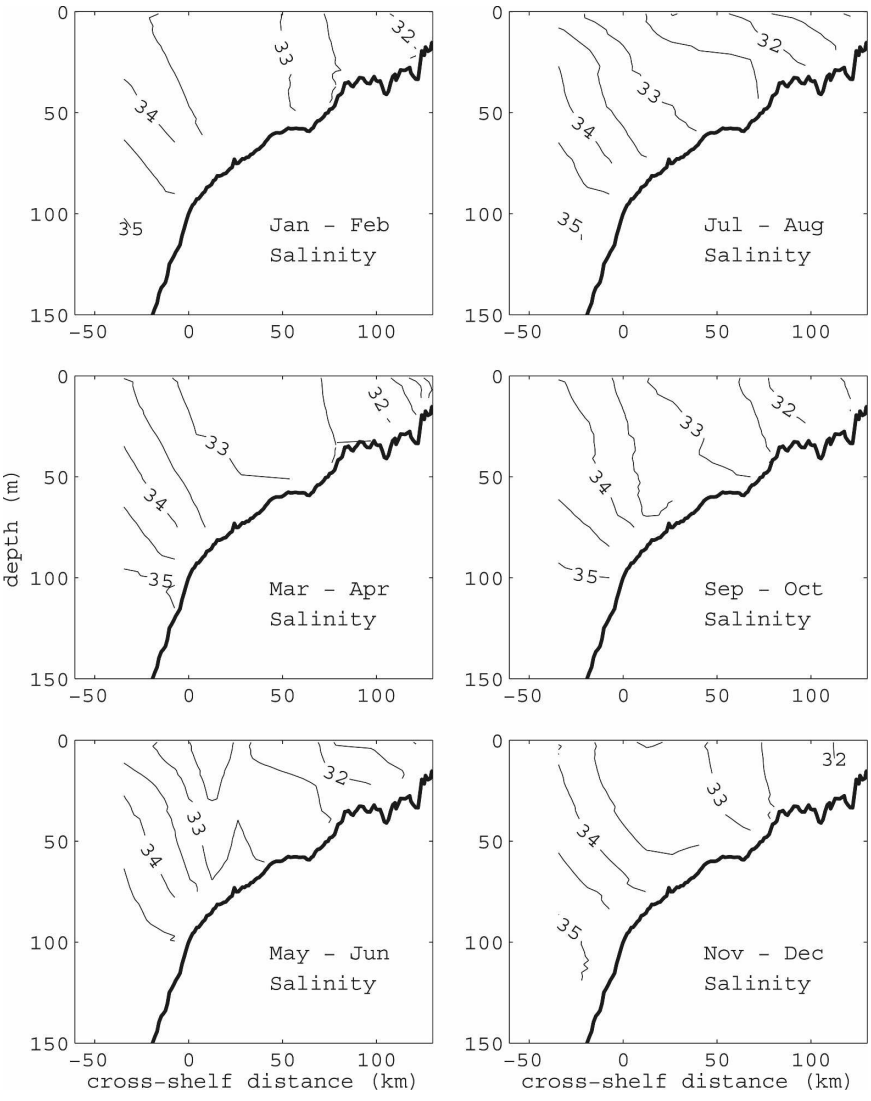

FIG. 9. Cross-shelf sections of bimonthly mean salinities for the New England shelf (69°–73°W).

cross-shelf temperature gradient enhances the cross-shelf salinity gradient (warmer and fresher water near the coast), resulting in an enhanced near-bottom cross-shelf density gradient. The larger cross-shelf density gradient implies an enhanced thermal wind shear and therefore an enhanced along-shelf flow. The maximum cross-shelf temperature gradient (temperature increasing onshore) occurs in July over the inner shelf. As the thermocline deepens, due to increasing wind events and decreasing surface heat flux in the autumn (Beardsley et al. 1985; Lentz et al. 2003), the maximum cross-shelf temperature gradient moves offshore (cf. July and September: Fig. 10). The maximum cross-shelf density gradient over the outer shelf, offshore of the center of the cold pool, occurs in late autumn (November), the only time of the year when the temperature does not increase offshore over the outer shelf. As a consequence of the seasonal evolution of the temperature field, the maximum cross-shelf density gradient near the bottom occurs in summer over the inner shelf, progressing to the outer shelf in late autumn, consistent with the progression observed south of Cape Cod and the fall maximum offshore of the 60-m isobath.

4. Summary

Seasonal variations in the depth-average (or interior) along-shelf flow are estimated for 27 sites with current time series longer than 200 days over the continental shelf of the Middle Atlantic Bight and southern flank of

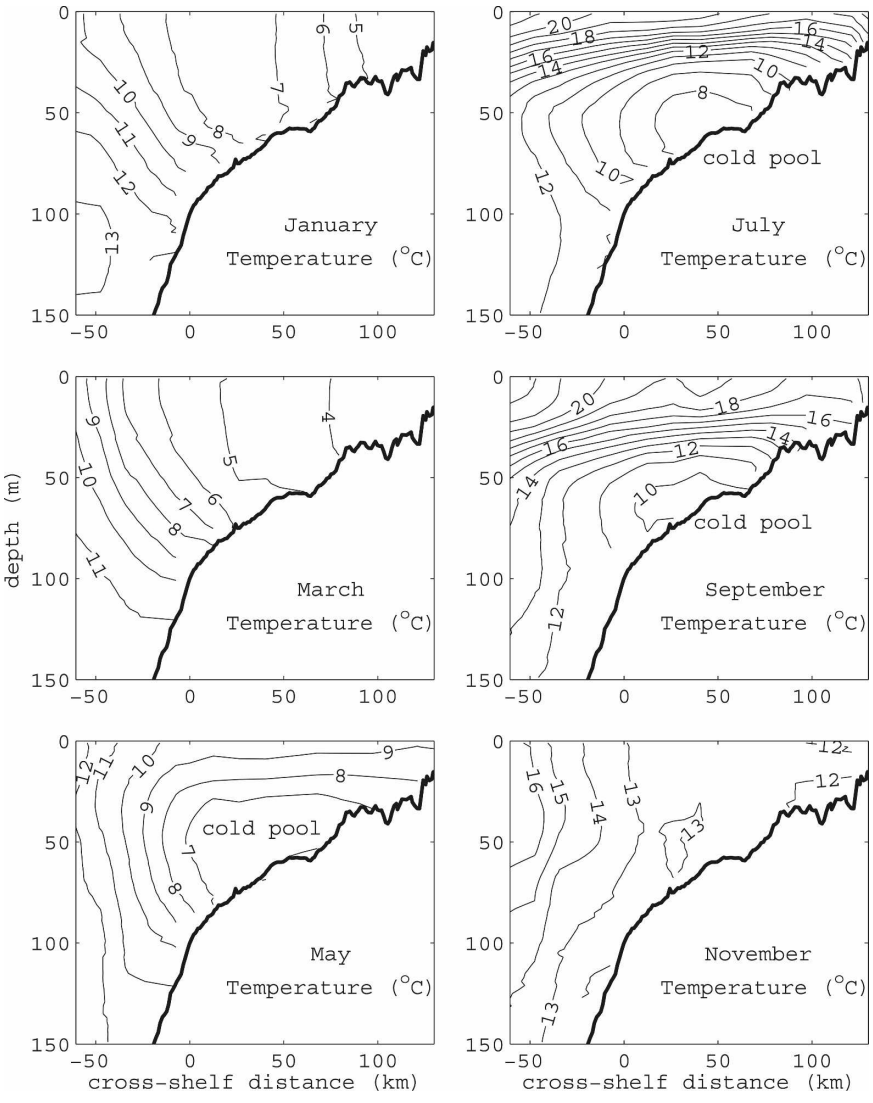

FIG. 10. As in Fig. 9, but of monthly mean temperatures, showing the seasonal evolution.

Georges Bank. Seasonal variations in the depth-average along-shelf flow are polarized along-isobath with major axis amplitudes of 1–5 cm s^{-1} (Fig. 1). The individual current time series are typically only about a year in duration and, hence, are not long enough to determine a reliable seasonal cycle. Nevertheless, the seasonal variations from the 27 sites exhibit some consistent patterns associated with seasonal variations in the wind stress, surface heat flux, and spring river discharge.

There is a significant, spatially uniform seasonal cycle in the wind stress with an amplitude of about 0.03–0.04 N m^{-2} polarized in the southeast–northwest direction (Fig. 2). However, the wind stress does not force a significant seasonal variation in the along-shelf flow over most of the MAB shelf and southern flank of Georges Bank (Fig. 6) because the orientation of the wind stress that forces the along-shelf flow is perpendicular to the orientation of the seasonal variation in the wind stress (Fig. 5b). There are significant seasonal variations in the wind-driven flow in the southern MAB (amplitude of 3 cm s^{-1}) and over the inner New England shelf (amplitude of 2 cm s^{-1}: see also Ullman and Codiga 2004; Codiga 2005) because there is a seasonal variation in the component of the wind stress that forces the flow in these regions.

When the wind-driven component of the flow is removed, there is a seasonal variation (1–5 cm s^{-1}) in the residual along-shelf flow with a phase such that the maximum equatorward flow tends to occur in spring onshore of the 60-m isobath and in autumn offshore of the 60-m isobath (Fig. 8b). The phase variation is con-

sistent with seasonal variations in the cross-shelf density gradient due to both salinity and temperature gradients. The maximum equatorward flow in spring onshore of the 60-m isobath is consistent with the maximum freshwater discharge from rivers and estuaries occurring in spring. The maximum equatorward flow in autumn offshore of the 60-m isobath and the steady phase increase with water depth offshore of Cape Cod are consistent with the seasonal variation in the near-bottom cross-shelf temperature (density) gradient. The seasonal variation in the cross-shelf temperature gradient is, in turn, associated with the development and destruction of a near-bottom pool of cold water over the mid and outer shelf ("cold pool") due to surface heating in spring–summer and surface cooling and wind-driven mixing in autumn–winter.

The seasonal variations in the depth-averaged alongshelf flow over the MAB shelf exhibit reasonable patterns that are sensible in the context of the seasonal variations in wind stress, surface heat flux, and river runoff. The sparse coverage and the large uncertainties in the seasonal variations emphasize the need for much longer time series with better spatial coverage to obtain a more complete picture of the seasonal variations in the circulation.

Acknowledgments. The author is grateful to the researchers (too numerous to list) who collected the historical data used here. The consistent pattern of weak seasonal variations in the circulation that emerged from this study is a testament to the care and effort that went into collecting these observations. The author also appreciates comments and suggestions on an early draft of this manuscript by Bob Beardsley, Ken Brink, and Melanie Fewings. The field programs were funded by Department of Energy, Minerals Management Service, National Science Foundation, National Oceanic and Atmospheric Administration, and the Office of Naval Research. This research was funded by the Ocean Sciences Division of the National Science Foundation under Grants OCE-820773, OCE-841292, and OCE-848961.

REFERENCES

Aikman, F., III, H. W. Ou, and R. W. Houghton, 1988: Current variability across the New England continental shelf-break and slope. *Cont. Shelf Res.,* **8,** 625–651.

Austin, J. A., and S. J. Lentz, 1999: The relationship between synoptic weather systems and meteorological forcing on the North Carolina inner shelf. *J. Geophys. Res.,* **104,** 18 159–18 186.

Beardsley, R. C., and W. C. Boicourt, 1981: On estuarine and continental-shelf circulation in the Middle Atlantic Bight. *Evolution of Physical Oceanography: Scientific Surveys in Honor of Henry Stommel,* B. A. Warren and C. Wunsch, Eds., The MIT Press, 198–233.

——, D. C. Chapman, K. H. Brink, S. R. Ramp, and R. Schlitz, 1985: The Nantucket Shoals Flux Experiment (NSFE79). Part I: A basic description of the current and temperature variability. *J. Phys. Oceanogr.,* **15,** 713–748.

Bigelow, H. B., 1933: Studies of the waters on the continental shelf, Cape Cod to Chesapeake Bay, I, The cycle of temperature. *Pap. Phys. Oceanogr. Meteor.,* **2,** 1–135.

——, and M. Sears, 1935: Studies of the waters on the continental shelf, Cape Cod to Chesapeake Bay, II, Salinity. *Pap. Phys. Oceanogr. Meteor.,* **4,** 1–94.

Brink, K. H., R. Limeburner, and R. C. Beardsley, 2003: Properties of flow and pressure over Georges Bank as observed with near-surface drifters. *J. Geophys. Res.,* **108,** 8001, doi:10.1029/2001JC001019.

Bumpus, D. F., 1973: A description of the circulation on the continental shelf of the east coast of the United States. *Prog. Oceanogr.,* **6,** 111–157.

Butman, B., 1987: Processes causing surficial sediment movement. *Georges Bank,* R. H. Backus, Ed., The MIT Press, 147–162.

——, and R. C. Beardsley, 1987: Long-term observations on the southern flank of Georges Bank. Part I: A description of the seasonal cycle of currents, temperature, stratification, and wind stress. *J. Phys. Oceanogr.,* **17,** 367–384.

Codiga, D. L., 2005: Interplay of wind forcing and buoyant discharge off Montauk Point: Seasonal changes to velocity structure and a coastal front. *J. Phys. Oceanogr.,* **35,** 1068–1085.

Flagg, C. N., 1987: Hydrographic structure and variability. *Georges Bank,* R. H. Backus, Ed., The MIT Press, 108–124.

——, and M. Dunn, 2003: Characterization of the mean and seasonal flow regime on Georges Bank from shipboard acoustic Doppler current profiler data. *J. Geophys. Res.,* **108,** 8002, doi:10.1029/2001JC001257.

——, ——, D.-P. Wang, H. T. Rossby, and R. L. Benway, 2006: A study of the currents of the outer shelf and upper slope from a decade of shipboard ADCP observations in the Middle Atlantic Bight. *J. Geophys. Res.,* **111,** C06003, doi:10.1029/2005JC003116.

Garvine, R. W., 2004: The vertical structure and subtidal dynamics of the inner shelf off New Jersey. *J. Mar. Res.,* **62,** 337–371.

Houghton, R. W., R. Schlitz, R. C. Beardsley, B. Butman, and J. L. Chamberlin, 1982: The Middle Atlantic Bight cold pool: Evolution of the temperature structure during summer, 1979. *J. Phys. Oceanogr.,* **12,** 1019–1029.

Isemer, H.-J., and L. Hasse, 1985: *Observations.* Vol. 1, *The Bunker Climate Atlas of the North Atlantic Ocean,* Springer-Verlag, 218 pp.

Kohut, J. T., S. M. Glenn, and R. J. Chant, 2004: Seasonal current variability on the New Jersey inner shelf. *J. Geophys. Res.,* **109,** C07S07, doi:10.1029/2003JC001963.

Large, W. G., and S. Pond, 1981: Open ocean momentum flux measurements in moderate to strong winds. *J. Phys. Oceanogr.,* **11,** 324–336.

Lentz, S. J., 2008: Observations and a model of the mean circulation over the Middle Atlantic Bight continental shelf. *J. Phys. Oceanogr.,* **38,** 1203–1221.

——, R. T. Guza, S. Elgar, F. Feddersen, and T. H. C. Herbers, 1999: Momentum balances on the North Carolina inner shelf. *J. Geophys. Res.,* **104,** 18 205–18 226.

——, K. Shearman, S. Anderson, A. Plueddemann, and J. Edson, 2003: The evolution of stratification over the New England shelf during the Coastal Mixing and Optics study, August

1996–June 1997. *J. Geophys. Res.,* **108,** 3008, doi:10.1029/2001JC001121.

Linder, C. A., and G. Gawarkiewicz, 1998: A climatology of the shelfbreak front in the Middle Atlantic Bight. *J. Geophys. Res.,* **103,** 18 405–18 423.

Manning, J., 1991: Middle Atlantic Bight salinity: Interannual variability. *Cont. Shelf Res.,* **11,** 123–137.

Mayer, D. A., D. V. Hansen, and D. A. Ortman, 1979: Long-term current and temperature observation on the Middle Atlantic shelf. *J. Geophys. Res.,* **84,** 1776–1792.

Mountain, D. G., 2003: Variability in the properties of shelf water in the Middle Atlantic Bight, 1977–1999. *J. Geophys. Res.,* **108,** 3014, doi:10.1029//2001JC001044.

Munchow, A., and R. W. Garvine, 1993: Dynamical properties of a buoyancy-driven coastal current. *J. Geophys. Res.,* **98,** 20 063–20 078.

Noble, M., B. Butman, and E. Williams, 1983: On the longshore structure and dynamics of subtidal currents on the eastern United States continental shelf. *J. Phys. Oceanogr.,* **13,** 2125–2147.

Pawlowicz, R., R. Beardsley, and S. J. Lentz, 2002: Classical tidal harmonic analysis with errors in MATLAB using T_TIDE. *Comput. Geosci.,* **28,** 929–937.

Rennie, S., J. L. Largier, and S. J. Lentz, 1999: Observations of low-salinity coastal current pulses downstream of Chesapeake Bay. *J. Geophys. Res.,* **104,** 18 227–18 240.

Saunders, P. M., 1977: Wind stress on the ocean over the eastern continental shelf of North America. *J. Phys. Oceanogr.,* **7,** 555–566.

Shearman, R. K., and S. J. Lentz, 2003: Dynamics of mean and subtidal flow on the New England shelf. *J. Geophys. Res.,* **108,** 3281, doi:10.1029/2002JC001417.

Ullman, D. S., and D. L. Codiga, 2004: Seasonal variation of a coastal jet in the Long Island Sound outflow region based on HF radar and Doppler current observations. *J. Geophys. Res.,* **109,** C07S06, doi:10.1029/2002JC001660.

Vickers, D., L. Mahrt, J. Sun, and T. Crawford, 2001: Structure of offshore flow. *Mon. Wea. Rev.,* **129,** 1251–1258.

Yankovsky, A. E., R. W. Garvine, and A. Munchow, 2000: Mesoscale currents on the inner New Jersey shelf driven by the interaction of buoyancy and wind forcing. *J. Phys. Oceanogr.,* **30,** 2214–2230.